

5. Rock mass properties

Introduction

Reliable estimates of the strength and deformation characteristics of rock masses are required for almost any form of analysis used for the design of slopes, foundations, and underground excavations. Hoek and Brown (1980a, 1980b) proposed a method for obtaining estimates of the strength of jointed rock masses, based upon an assessment of the interlocking of rock blocks and the condition of the surfaces between these blocks. This method was modified over the years to meet the needs of users who were applying it to problems that were not considered when the original criterion was developed (Hoek 1983, and Hoek and Brown 1988). The application of the method to very poor-quality rock masses required further changes (Hoek, Wood, and Shah 1992) and, eventually, the development of a new classification called the Geological Strength Index (Hoek, Kaiser and Bawden 1995, Hoek 1994, Hoek and Brown 1997, Hoek, Marinos and Benissi, 1998, Marinos and Hoek, 2001) was developed. A major revision was carried out in 2002 to smooth out the curves, necessary for the application of the criterion in numerical models, and to update the methods for estimating Mohr Coulomb parameters (Hoek, Carranza-Torres and Corkum, 2002). A related modification for estimating the deformation modulus of rock masses was made by Hoek and Diederichs (2006). The most recent and probably final version of the criterion was published by Hoek and Brown (2019).

This chapter presents the Hoek-Brown criterion in a form that has been found to be practical in the field and provide the most reliable set of results to use as input for the methods of analysis in current use in rock engineering.

Generalised Hoek-Brown criterion

The Generalised Hoek-Brown failure criterion for jointed rock masses is defined by:

$$\sigma'_1 = \sigma'_3 + \sigma_{ci} \left(m_b \frac{\sigma'_3}{\sigma_{ci}} + s \right)^a \quad (1)$$

where σ'_1 and σ'_3 are the maximum and minimum effective principal stresses at failure, m_b is the value of the Hoek-Brown constant m for the rock mass, s and a are constants which depend upon the rock mass characteristics, and σ_{ci} is the uniaxial compressive strength of the intact rock pieces.

Normal and shear stresses are related to principal stresses by the equations originally published by Balmer (1952).

$$\sigma'_n = \frac{\sigma'_1 + \sigma'_3}{2} - \frac{\sigma'_1 - \sigma'_3}{2} \cdot \frac{d\sigma'_1/d\sigma'_3 - 1}{d\sigma'_1/d\sigma'_3 + 1} \quad (2)$$

$$\tau = (\sigma'_1 - \sigma'_3) \frac{\sqrt{d\sigma'_1/d\sigma'_3}}{d\sigma'_1/d\sigma'_3 + 1} \quad (3)$$

$$\text{where } d\sigma'_1/d\sigma'_3 = 1 + am_b(m_b\sigma'_3/\sigma_{ci} + s)^{a-1} \quad (4)$$

To use the Hoek-Brown criterion for estimating the strength and deformability of jointed rock masses, three properties of the rock mass must be estimated. These are:

- uniaxial compressive strength σ_{ci} of the intact rock pieces,
- value of the Hoek-Brown constant m_i for these intact rock pieces, and
- value of the Geological Strength Index GSI for the rock mass.

Figure 1 presents a summary of estimates of the uniaxial compressive strength of rock and comments on the estimation of these values in the field. Figure 2 presents a more comprehensive summary of values of deformation modulus, uniaxial compressive strength, and the Hoek-Brown constant m_i for intact rock specimens. These summaries can be used as a starting point in the estimation of rock mass strengths.

Anisotropic and foliated rocks such as slates, schists and phyllites, the behaviour of which is dominated by closely spaced planes of weakness, cleavage or schistosity, present difficulties in the determination of the uniaxial compressive strengths.

Salcedo (1983) has published the results of a set of directional uniaxial compressive tests on a graphitic phyllite from Venezuela. These results showed that the uniaxial compressive strength of this material varies by a factor of about 5, depending upon the direction of loading.

In deciding upon the value of σ_{ci} for foliated rocks, a decision must be made on whether to use the highest or the lowest uniaxial compressive strength obtained from tests. Mineral composition, grain size, grade of metamorphism and tectonic history all play a role in determining the characteristics of the rock mass. The author cannot offer any detailed guidance on the choice of σ_{ci} , but insight into the role of schistosity in rock masses can be obtained by considering the case of the Yacambú-Quibor tunnel in Venezuela.

Grade*	Term	Uniaxial Comp. Strength (MPa)	Point Load Index (MPa)	Field estimate of strength	Examples
R6	Extremely Strong	> 250	>10	Specimen can only be chipped with a geological hammer	Fresh basalt, chert, diabase, gneiss, granite, quartzite
R5	Very strong	100 - 250	4 - 10	Specimen requires many blows of a geological hammer to fracture it	Amphibolite, sandstone, basalt, gabbro, gneiss, granodiorite, limestone, marble, rhyolite, tuff
R4	Strong	50 - 100	2 - 4	Specimen requires more than one blow of a geological hammer to fracture it	Limestone, marble, phyllite, sandstone, schist, shale
R3	Medium strong	25 - 50	1 - 2	Cannot be scraped or peeled using a pocketknife, specimen can be fractured with a single blow from a geological hammer	Claystone, coal, concrete, schist, shale, siltstone
R2	Weak	5 - 25	**	Can be peeled with a pocketknife with difficulty, shallow indentation made by firm blow with point of a geological hammer	Chalk, rocksalt, potash
R1	Very weak	1 - 5	**	Crumbles under firm blows with point of a geological hammer, can be peeled by a pocketknife	Highly weathered or altered rock
R0	Extremely weak	0.25 - 1	**	Indented by thumbnail	Stiff fault gouge

* Grade according to Brown (1981).

** Point load tests on rocks with a uniaxial compressive strength below 25 MPa are likely to yield highly ambiguous results.

Figure 1: estimates of uniaxial compressive strength.



Figure 3: Yacambú-Quibor graphitic phyllite in the tunnel face.

The Yacambú-Quibor tunnel, discussed in a later chapter, was excavated in graphitic phyllite at depths of up to 1200 m in the Andes Mountains in Venezuela. The appearance of the rock mass at the tunnel face is shown in Figure 3. Back analysis of the behaviour of this material suggests that an appropriate value for σ_{ci} is approximately 50 MPa. In other words, on the scale of the 5.5 m diameter tunnel, the rock mass properties are “averaged” and there is no sign of anisotropic behaviour in the deformations measured in the tunnel.

Influence of sample size

The influence of sample size upon rock strength has been widely discussed in geotechnical literature and it is generally assumed that there is a significant reduction in strength with increasing sample size. Based upon an analysis of published data, Hoek and Brown (1980a) have suggested that the uniaxial compressive strength σ_{cd} of a rock specimen with a diameter of d mm is related to the uniaxial compressive strength σ_{c50} of a 50 mm diameter sample by the following relationship:

$$\sigma_{cd} = \sigma_{c50} \left(\frac{50}{d} \right)^{0.18} \quad (5)$$

This relationship, together with the data upon which it was based, is shown in Figure 4.

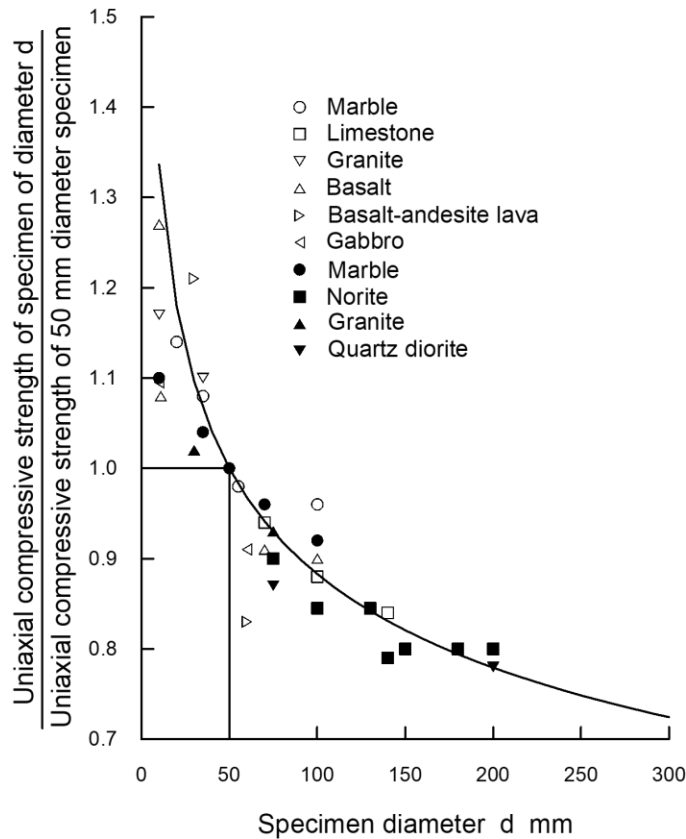


Figure 4: Influence of specimen size on the strength of intact rock. Hoek and Brown (1980a).

It is suggested that the reduction in strength is due to the greater opportunity for failure through and around grains, the ‘building blocks’ of the intact rock, as more and more of these grains are included in the test sample. Eventually, when a sufficiently large number of grains are included in the sample, the strength reaches a constant value.

The Hoek-Brown failure criterion, which assumes isotropic rock and rock mass behaviour, should only be applied to those rock masses in which many closely spaced discontinuities exist, such that isotropic behaviour involving failure on discontinuities can be assumed. When the structure being analysed is large and the block size small in comparison, the rock mass can be treated as a Hoek-Brown material.

Where the block size is of the same order as that of the structure being analysed, or when one of the discontinuity sets is significantly weaker than the others, the Hoek-Brown criterion should not be used. In these cases, the stability of the structure should be analysed by considering failure mechanisms involving the sliding or rotation of blocks and wedges defined by intersecting structural features.

It is reasonable to extend this argument to suggest that, when dealing with large scale rock masses, the strength will reach a constant value when the size of individual rock pieces is small in relation to the overall size of the structure being considered. This suggestion is embodied in Figure 5 which shows the transition from an isotropic intact rock specimen, through a highly anisotropic rock mass in which failure is controlled by one or two discontinuities, to an isotropic heavily jointed rock mass.

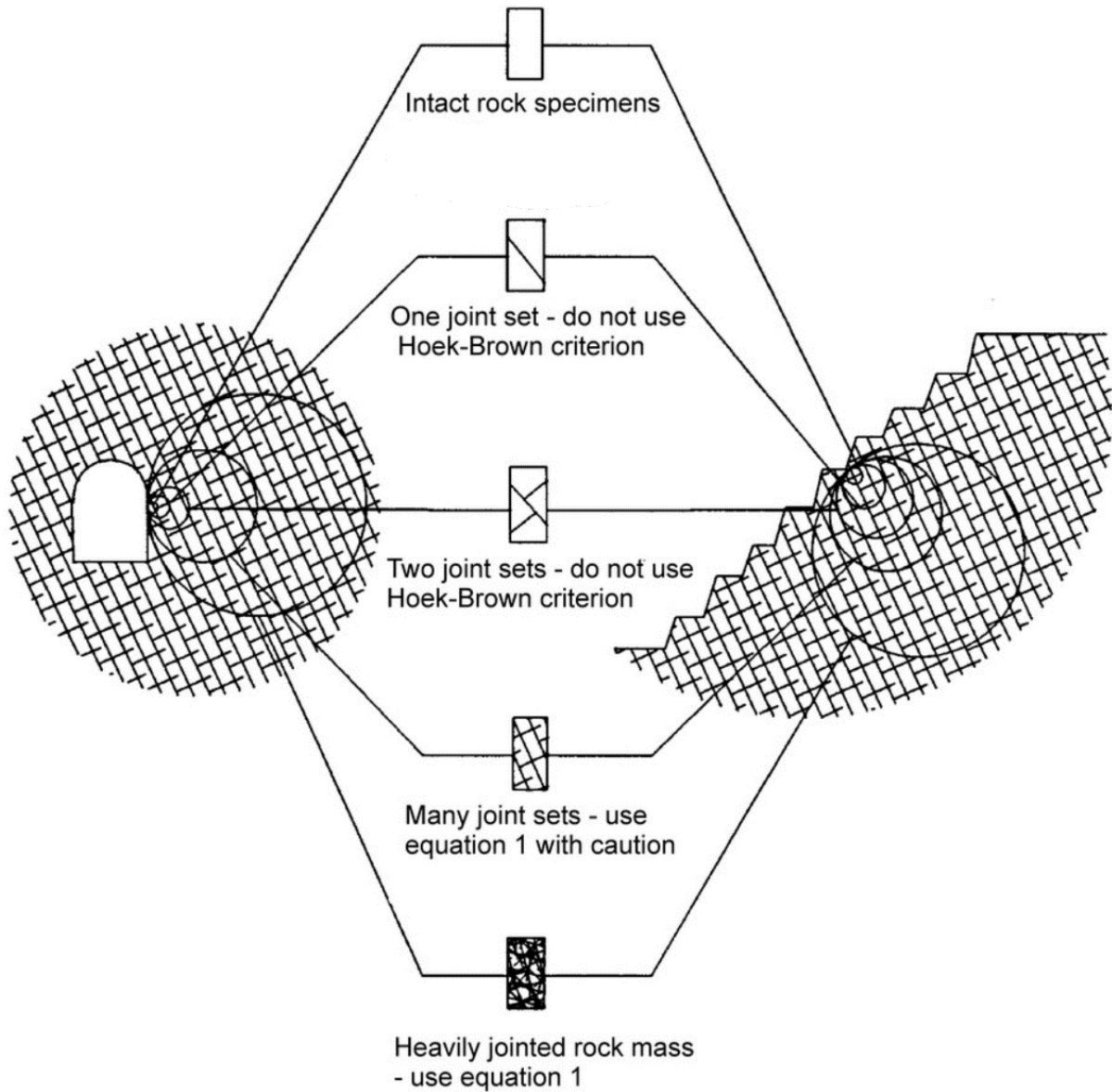


Figure 5: Idealised diagram showing the transition from intact to a heavily jointed rock mass with increasing sample size.

Geological Strength Index

The strength of a jointed rock mass depends on the properties of the intact rock pieces and the freedom of these pieces to slide and rotate under different stress conditions. This freedom depends on the geometrical shape of the intact rock pieces as well as the condition of the surfaces separating the pieces. Angular rock pieces with clean, rough discontinuity surfaces will result in a much stronger rock mass than one which contains rounded particles surrounded by weathered and altered material.

The Geological Strength Index (GSI), introduced by Hoek (1994) and Hoek, Kaiser and Bawden (1995) provides a number which, when combined with the intact rock properties, can be used for estimating the reduction in rock mass strength for different geological conditions. This system is presented in Figure 6, for blocky rock masses, and Figure 7 for heterogeneous rock masses such as flysch. Figure 7 has also been extended to deal with molassic rocks (Hoek et al, 2006) and ophiolites (Marinos et al, 2005).

Before the introduction of the GSI system in 1994, the application of the Hoek-Brown criterion in the field was based on a correlation with the 1976 version of Bieniawski's Rock Mass Rating (RMR), with the Groundwater Rating set to 10 (dry) and the Adjustment for Joint Orientation set to 0 (very favourable) (Bieniawski, 1976). If the 1989 version of RMR (Bieniawski, 1989) is used, then the Groundwater Rating is set to 15 and the Adjustment for Joint Orientation set to zero.

During the early years the value of GSI was estimated directly from RMR. However, this correlation has proved to be unreliable, particularly for poor quality rock masses and for rocks with lithological peculiarities that cannot be accommodated in the RMR classification. Consequently, it is recommended that GSI should be estimated directly by means of the charts presented in Figures 6 and 7 and not from the RMR classification.

Experience shows that most geologists and engineering geologists are comfortable with the descriptive and largely qualitative nature of the GSI tables and generally have little difficulty in arriving at an estimated value. On the other hand, many engineers feel the need for a more quantitative system in which they can "measure" some physical dimension. Conversely, these engineers have little difficulty understanding the importance of the intact rock strength σ_{ci} and its incorporation in the assessment of the rock mass properties.

Many geologists tend to confuse intact and rock mass strength and consistently underestimate the intact strength.

An additional practical question is whether borehole cores can be used to estimate the GSI value behind the visible faces. Borehole cores are the best source of data at depth, but it must be recognized that it is necessary to extrapolate the one-dimensional information provided by core to the three-dimensional rock mass. However, this is a common problem in borehole investigation and most experienced engineering geologists are comfortable with this extrapolation process. Multiple boreholes and inclined boreholes are of great help in the interpretation of rock mass characteristics at depth.

<p>GEOLOGICAL STRENGTH INDEX FOR JOINTED ROCKS (Hoek and Marinos, 2000)</p> <p>From the lithology, structure and surface conditions of the discontinuities, estimate the average value of GSI. Do not try to be too precise. Quoting a range from 33 to 37 is more realistic than stating that GSI = 35. Note that the table does not apply to structurally controlled failures. Where weak planar structural planes are present in an unfavourable orientation with respect to the excavation face, these will dominate the rock mass behaviour. The shear strength of surfaces in rocks that are prone to deterioration as a result of changes in moisture content will be reduced if water is present. When working with rocks in the fair to very poor categories, a shift to the right may be made for wet conditions. Water pressure is dealt with by effective stress analysis.</p>		SURFACE CONDITIONS				
STRUCTURE		DECREASING SURFACE QUALITY →				
		VERY GOOD Very rough, fresh unweathered surfaces	GOOD Rough, slightly weathered, iron stained surfaces	FAIR Smooth, moderately weathered and altered surfaces	POOR Slickensided, highly weathered surfaces with compact coatings or fillings or angular fragments	VERY POOR Slickensided, highly weathered surfaces with soft clay coatings or fillings
	INTACT OR MASSIVE - intact rock specimens or massive in situ rock with few widely spaced discontinuities	90			N/A	N/A
	BLOCKY - well interlocked undisturbed rock mass consisting of cubical blocks formed by three intersecting discontinuity sets	80	70			
	VERY BLOCKY- interlocked, partially disturbed mass with multi-faceted angular blocks formed by 4 or more joint sets		60	50		
	BLOCKY/DISTURBED/SEAMY - folded with angular blocks formed by many intersecting discontinuity sets. Persistence of bedding planes or schistosity			40	30	
	DISINTEGRATED - poorly interlocked, heavily broken rock mass with mixture of angular and rounded rock pieces				20	
	LAMINATED/SHEARED - Lack of blockiness due to close spacing of weak schistosity or shear planes	N/A	N/A			10

Figure 6: Characterisation of blocky rock masses based on interlocking and joint conditions.

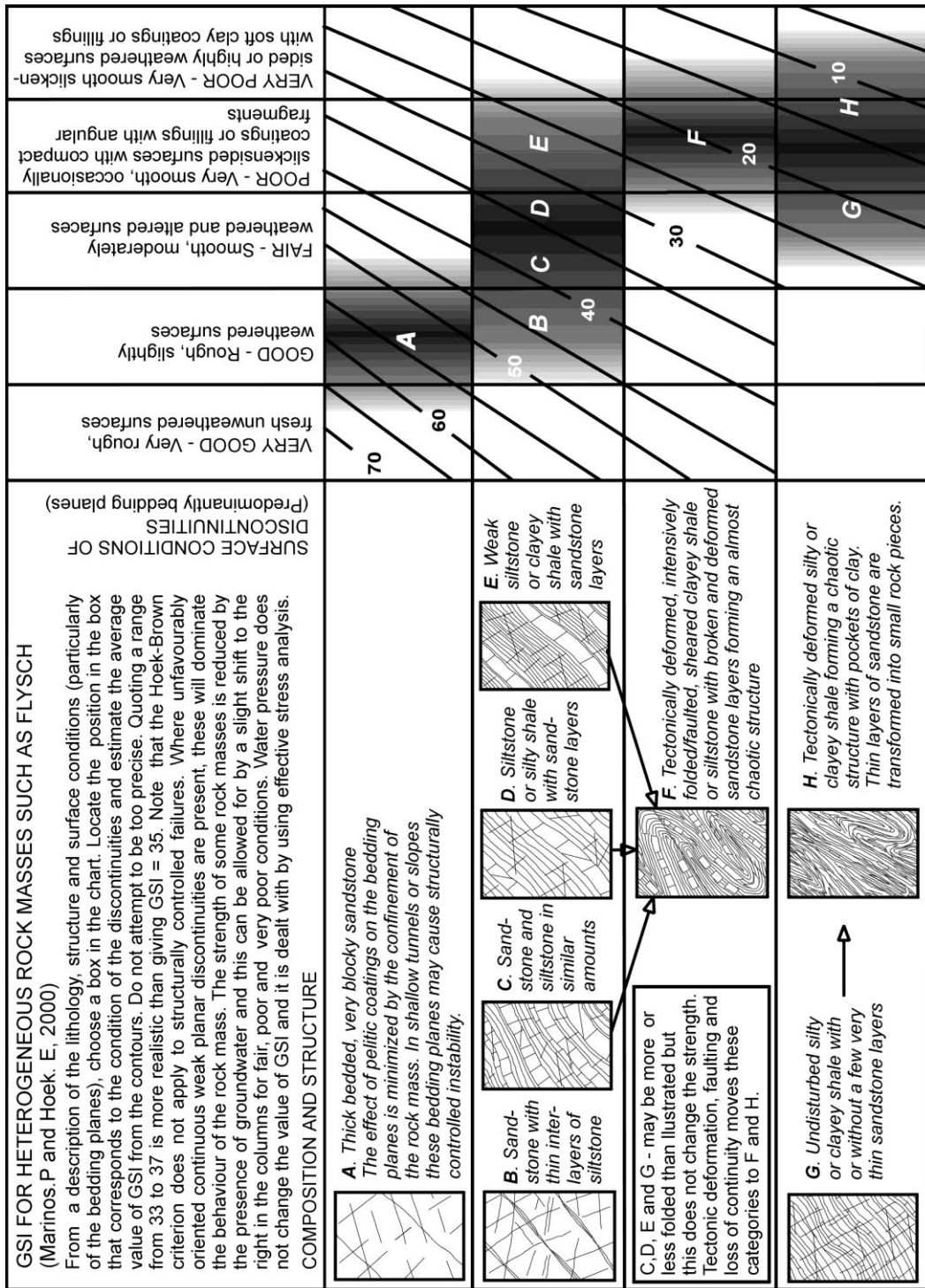


Figure 7: Estimate of Geological Strength Index GSI for heterogeneous rock masses, such as flysch. (After Marinos and Hoek, 2001).

The most important decision to be made in using the GSI system is whether it should be used. If the discontinuity spacing is large compared with the dimensions of the tunnel or slope under consideration then, as shown in Figure 5, the GSI tables and the Hoek-Brown criterion should not be used, and the discontinuities should be treated individually. Where the discontinuity spacing is small compared with the size of the structure (bottom of Figure 5) then the GSI tables can be used with confidence.

One of the practical problems that arises when assessing the value of GSI in the field is related to blast damage. As illustrated in Figure 8, there is a considerable difference in the appearance of a rock face which has been excavated by controlled blasting and a face which has been damaged by bulk blasting. Wherever possible, the undamaged face should be used to estimate the value of GSI since the overall aim is to determine the properties of the undisturbed rock mass.



Figure 8: Comparison between the results achieved using controlled blasting (on the left) and normal bulk blasting for a surface excavation in gneiss.

The influence of blast damage on the near surface rock mass properties has been considered in the 2002 version of the Hoek-Brown criterion (Hoek, Carranza-Torres and Corkum (2002)).

$$m_b = m_i \exp\left(\frac{GSI-100}{28-14D}\right) \quad (6)$$

$$s = \exp\left(\frac{GSI - 100}{9 - 3D}\right) \quad (7)$$

$$a = \frac{1}{2} + \frac{1}{6} (e^{-GSI/15} - e^{-20/3}) \quad (8)$$

D is a factor which depends upon the degree of disturbance due to blast damage and stress relaxation. It varies from 0 for undisturbed in situ rock masses to 1 for very disturbed rock masses. Guidelines for the selection of D are presented in Figure 9.

Note that the factor D applies only to the blast damaged zone. It should not be applied to the entire rock mass. For example, in tunnels the blast damage is generally limited to a 1 to 2 m thick zone around the tunnel, and this should be incorporated into numerical models as a different and weaker material than the surrounding rock mass. Applying the blast damage factor D to the entire rock mass is inappropriate and can result in misleading and unnecessarily pessimistic results.

The uniaxial compressive strength of the rock mass is obtained by setting $\sigma'_3 = 0$ in equation 1, giving:

$$\sigma_c = \sigma_{ci} \cdot s^a \quad (9)$$

and the tensile strength of the rock mass is:

$$\sigma_t = -\frac{s\sigma_{ci}}{m_b} \quad (10)$$

Equation 15, on page 16, is obtained by setting $\sigma'_1 = \sigma'_3 = \sigma_t$ in equation 1. This represents a condition of biaxial tension. Hoek (1983) showed that, for brittle materials, the uniaxial tensile strength is equal to the biaxial tensile strength.

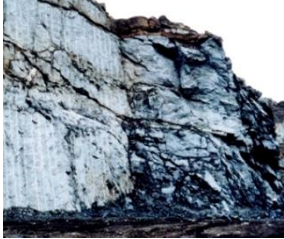
Appearance of rock	Description of rock mass	Suggested D value
	Excellent quality-controlled blasting or excavation by Tunnel Boring Machine results in minimal disturbance to the confined rock mass surrounding a tunnel.	D = 0
	Mechanical or hand excavation in poor quality rock masses (no blasting) results in minimal disturbance to the surrounding rock mass. Where squeezing problems result in significant floor heave, disturbance can be severe unless a temporary invert, as shown in the photograph, is placed.	Mechanical excavation D = 0 No invert D = 0.5
	Very poor-quality blasting in a hard rock tunnel results in severe local damage, extending 2 or 3 m, in the surrounding rock mass.	D = 0.8
	Small scale blasting in civil engineering slopes results in modest rock mass damage, particularly if controlled blasting is used as shown on the left-hand side of the photograph. However, stress relief results in some disturbance.	D = 0.7 Good blasting D = 1.0 Poor blasting
	Very large open pit mine slopes suffer significant disturbance due to heavy production blasting and also due to stress relief from overburden removal. In some softer rocks excavation can be carried out by ripping and dozing and the degree of damage to the slopes is less.	D = 1.0 Production blasting D = 0.7

Figure 9: Guidelines for estimating the disturbance factor D.

Note that the “switch” at $GSI = 25$ for the coefficients s and a (Hoek and Brown, 1997) has been eliminated in equations 9 and 10, giving a smooth continuous transition for the entire range of GSI values. The numerical values of s and a , given by these equations, are remarkably close to those given by the previous equations and it is not necessary for readers to revisit and make corrections to old calculations.

Mohr-Coulomb parameters

Since many geotechnical software programs are written in terms of the Mohr-Coulomb failure criterion, it is sometimes necessary to determine equivalent angles of friction and cohesive strengths for each rock mass and stress range. This is done by fitting an average linear relationship to the curve generated by solving equation 1 for a range of minor principal stress values defined by $\sigma_t < \sigma_3 < \sigma_{3max}$, as illustrated in Figure 10. The fitting process involves balancing the areas above and below the Mohr-Coulomb plot. This results in the following equations for the angle of friction φ' and cohesive strength c' :

$$\varphi' = \sin^{-1} \left[\frac{6am_b(s+m_b\sigma'_{3n})^{a-1}}{2(1+a)(2+a)+6am_b(s+m_b\sigma'_{3n})^{a-1}} \right] \quad (11)$$

$$c' = \frac{\sigma_{ci}[(1+2a)s + (1-a)m_b\sigma'_{3n}](s+m_b\sigma'_{3n})^{a-1}}{(1+a)(2+a)\sqrt{1+(6am_b(s+m_b\sigma'_{3n})^{a-1})/((1+a)(2+a))}} \quad (12)$$

where $\sigma_{3n} = \sigma'_{3max}/\sigma_{ci}$

Note that the value of σ'_{3max} , the upper limit of confining stress over which the relationship between the Hoek-Brown and the Mohr-Coulomb criteria is considered, must be determined for each individual case. Guidelines for selecting these values for slopes as well as shallow and deep tunnels are presented later.

The Mohr-Coulomb shear strength τ , for a given normal stress σ , is found by substitution of these values of c' and φ' into the equation:

$$\tau = c' + \sigma \tan \varphi' \quad (13)$$

The equivalent plot, in terms of the major and minor principal stresses, is defined by:

$$\sigma'_1 = \frac{2c' \cos \varphi'}{1 - \sin \varphi'} + \frac{1 + \sin \varphi'}{1 - \sin \varphi'} \sigma'_3 \quad (14)$$

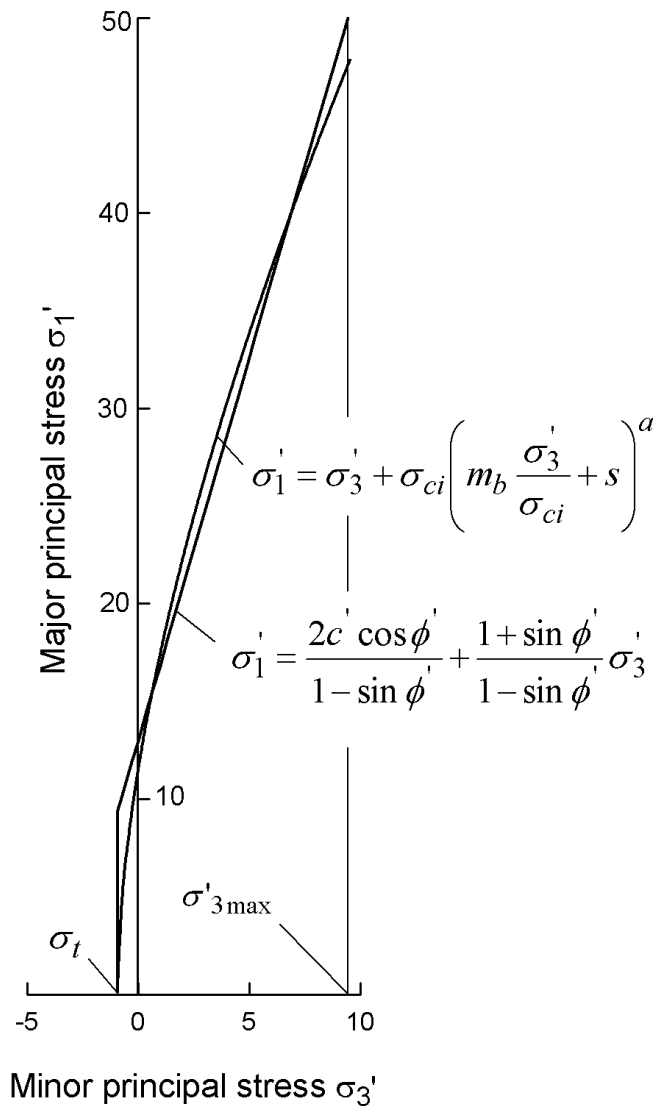


Figure 10: Relationships between major and minor principal stresses for Hoek-Brown and the equivalent Mohr-Coulomb criteria.

Rock mass strength

The uniaxial compressive strength of the rock mass σ_c is given by equation 9. Failure initiates at the boundary of an excavation when σ_c is exceeded by the stress induced on that boundary. The failure propagates from this initiation point into a biaxial stress field and it eventually stabilizes when the local strength, defined by equation 1, is higher than the induced stresses σ'_1 and σ'_3 . Most numerical models can follow this process of fracture propagation and this level of detailed analysis is very important when considering the stability of excavations in rock and when designing support systems.

However, there are times when it is useful to consider the overall behaviour of a rock mass rather than the detailed failure propagation process described above. For example, when considering the strength of a pillar, it is useful to have an estimate of the overall strength of the pillar rather than a detailed evaluation of the extent of fracture propagation in the pillar. This leads to the concept of a global “rock mass strength” and Hoek and Brown (1997) proposed that this could be estimated from the Mohr-Coulomb relationship:

$$\sigma'_{cm} = \frac{2c' \cos \varphi'}{1 - \sin \varphi'} \quad (15)$$

with c' and φ' determined for the stress range $\sigma_t < \sigma'_3 < \sigma_{ci}/4$ giving

$$\sigma'_{cm} = \sigma_{ci} \cdot \frac{(m_b + 4s - a(m_b - 8s))(m_b/4 + s)^{a-1}}{2(1+a)(2+a)} \quad (16)$$

Determination of σ'_{3max}

The issue of determining the appropriate value of σ'_{3max} for use in equations 11 and 12 depends upon the specific application. Two cases will be investigated:

Tunnels – where the value of σ'_{3max} is that which gives equivalent characteristic curves for the two failure criteria for deep tunnels or equivalent subsidence profiles for shallow tunnels.

Slopes – here the calculated factor of safety and the shape and location of the failure surface must be equivalent.

For the case of deep tunnels, solutions for both the Generalized Hoek-Brown and the Mohr-Coulomb criteria have been used to generate hundreds of solutions and to find the value of σ'_{3max} that gives equivalent characteristic curves. For shallow tunnels, where the depth below surface is less than 3 tunnel diameters, comparative numerical studies of the extent of failure and the magnitude of surface subsidence gave an identical relationship to that obtained for deep tunnels if caving to surface is avoided.

The results of the studies for deep tunnels are plotted in Figure 11 and the fitted equation for both shallow and deep tunnels is:

$$\frac{\sigma'_{3max}}{\sigma'_{cm}} = 0.47 \left(\frac{\sigma'_{cm}}{\gamma H} \right)^{-0.94} \quad (17)$$

where σ'_{cm} is the rock mass strength, defined by equation 21, γ is the unit weight of the rock mass and H is the depth of the tunnel below surface. In cases where the horizontal stress is higher than the vertical stress, the horizontal stress value should be used in place of γH .

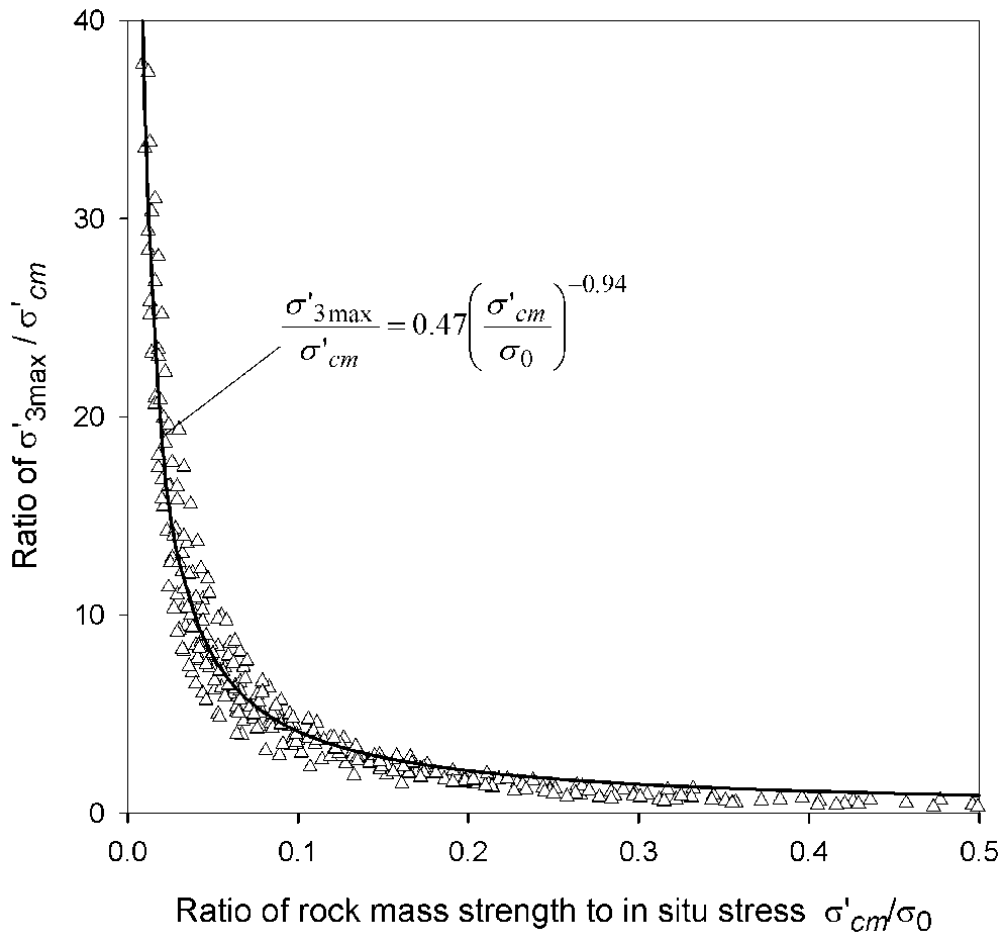


Figure 11: Relationship for the calculation of σ'_{3max} for equivalent Mohr-Coulomb and Hoek-Brown parameters for tunnels.

Equation 17 applies to all underground excavations, which are surrounded by a zone of failure that does not extend to surface. For studies of problems such as block caving in mines, it is recommended that no attempt should be made to relate the Hoek-Brown and Mohr-Coulomb parameters and that the determination of material properties and subsequent analysis should be based on only one of these criteria.

Similar studies for slopes, using Bishop's circular failure analysis for a wide range of slope geometries and rock mass properties, gave:

$$\frac{\sigma'_{3max}}{\sigma'_{cm}} = 0.72 \left(\frac{\sigma'_{cm}}{\gamma H} \right)^{-0.91} \quad (18)$$

Where H is the height of the slope.

Deformation modulus

Hoek and Diederichs (2006) re-examined existing empirical methods for estimating rock mass deformation modulus and concluded that none of these methods provided reliable estimates over the entire range of rock mass conditions encountered. Large errors were found for very poor rock masses and, at the other end of the spectrum, for massive strong rock masses. Fortunately, a new set of reliable measured data from China and Taiwan was available for analyses and it was found that the equation which gave the best fit to this data is a sigmoid function having the form:

$$y = c + \frac{a}{1 + e^{-((x-x_0)/b)}} \quad (19)$$

Using commercial curve fitting software, Equation 19 was fitted to the Chinese and Taiwanese data and the constants a and b in the fitted equation were then replaced by expressions incorporating GSI and the disturbance factor D . These were adjusted to give the equivalent average curve and the upper and lower bounds into which > 90% of the data points fitted. Note that the constant $a = 100\,000$ in Equation 20 is a scaling factor which is not directly related to the physical properties of the rock mass.

The following best-fit equation was derived:

$$E_{rm}(MPa) = 100000 \left(\frac{1-D/2}{1 + e^{((75+25D-GSI)/11)}} \right) \quad (20)$$

The rock mass deformation modulus data from China and Taiwan includes information on the geology as well as the uniaxial compressive strength (σ_{ci}) of the intact rock. This information permits a more detailed analysis in which the ratio of mass to intact modulus (E_{rm}/E_i) can be included. Using the modulus ratio MR proposed by Deere (1968) (modified by the authors based in part on this data set and on additional correlations from Palmstrom and Singh (2001)), it is possible to estimate the intact modulus from:

$$E_i = MR \cdot \sigma_{ci} \quad (21)$$

This relationship is useful when no direct values of the intact modulus (E_i) are available or where completely undisturbed sampling for measurement of E_i is difficult. A detailed analysis of the Chinese and Taiwanese data, using Equation (21) to estimate E_i resulted in the following equation:

$$E_{rm} = E_i \left(0.02 + \frac{1-D/2}{1 + e^{((60+15D-GSI)/11)}} \right) \quad (22)$$

This equation incorporates a finite value for the parameter c (Equation 19) to account for the modulus of broken rock (transported rock, aggregate or soil) described by $GSI = 0$. This equation is plotted against the average normalized field data from China and Taiwan in Figure 12.

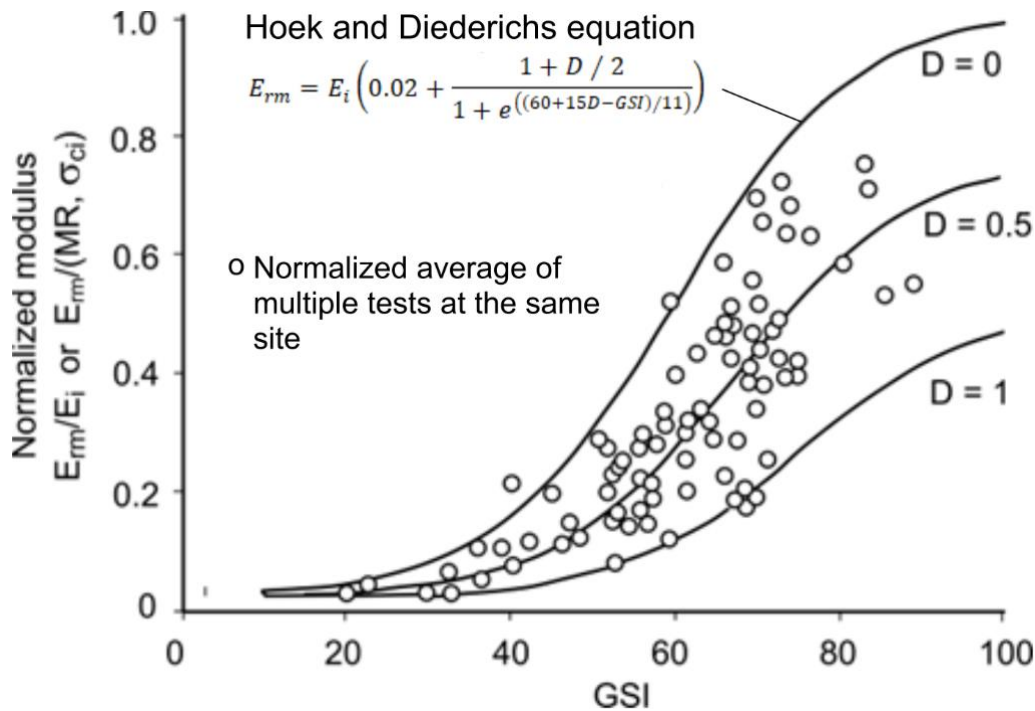


Figure 12: Plot of normalized in situ rock mass deformation modulus from China and Taiwan against Hoek and Diederichs Equation (22). Each data point represents the average of multiple tests at the same site in the same rock mass.

Figure 13, based on the modulus ratio (MR) values proposed by Deere (1968) can be used for calculating the intact rock modulus E_i . In general, measured values of E_i are seldom available and, even when they are, their reliability is suspect because of specimen damage. This specimen damage has a greater impact on modulus than on strength and, hence, the intact rock strength, when available, can usually be considered more reliable for use in equation (21).

Post-failure behaviour

When using numerical models to study the progressive failure of rock masses, estimates of the post-peak or post-failure characteristics of the rock mass are required. In some of these models, the Hoek-Brown failure criterion is treated as a yield criterion and the analysis is carried out using plasticity theory. No definite rules for dealing with this problem can be given but based upon experience in numerical analysis of a variety of practical problems, the post-failure characteristics, illustrated in Figure 14, are suggested as a starting point.

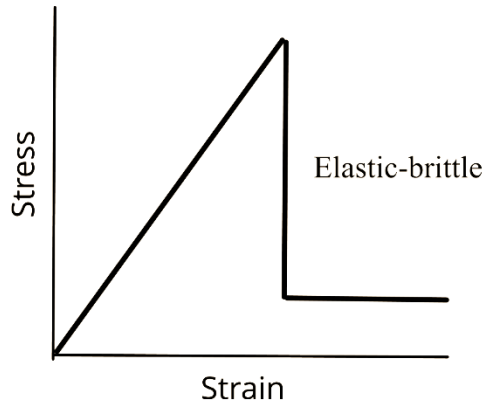
	Class	Group	Texture			
			Coarse	Medium	Fine	Very fine
SEDIMENTARY	Clastic		Conglomerates 300-400	Sandstones 200-350	Siltstones 350-400	Claystones 200-300
			Breccias 230-350		Greywackes 350	Shales 150-250 * Marls 150-200
	Non-Clastic	Carbonates	Crystalline Limestone 400-600	Sparitic Limestones 600-800	Micritic Limestones 800-1000	Dolomites 350-500
		Evaporites		Gypsum (350)**	Anhydrite (350)**	
		Organic			Chalk 1000+	
METAMORPHIC	Non Foliated		Marble 700-1000	Hornfels 400-700 Metasandstone 200-300	Quartzites 300-450	
	Slightly foliated		Migmatite 350-400	Amphibolites 400-500	Gneiss 300-750*	
	Foliated*			Schists 250-1100*	Phyllites /Mica Schist 300-800*	Slates 400-600*
IGNEOUS	Plutonic	Light	Granite+ 300-550	Diorite+ 300-350 Granodiorite+ 400-450		
		Dark	Gabbro 400-500 Norite 350-400	Dolerite 300-400		
	Hypabyssal		Porphyries (400)**		Diabase 300-350	Peridotite 250-300
	Volcanic	Lava		Rhyolite 300-500 Andesite 300-500	Dacite 350-450 Basalt 250-450	
		Pyroclastic	Agglomerate 400-600	Volcanic breccia (500)**	Tuff 200-400	

* Highly anisotropic rocks: the value of MR will be significantly different if normal strain and/or loading occurs parallel (high MR) or perpendicular (low MR) to a weakness plane. Uniaxial test loading direction should be equivalent to field application.

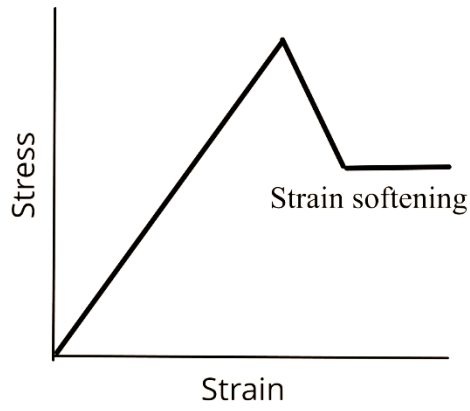
+ Felsic Granitoids: Coarse Grained or Altered (high MR), fined grained (low MR).

** No data available, estimated on the basis of geological logic.

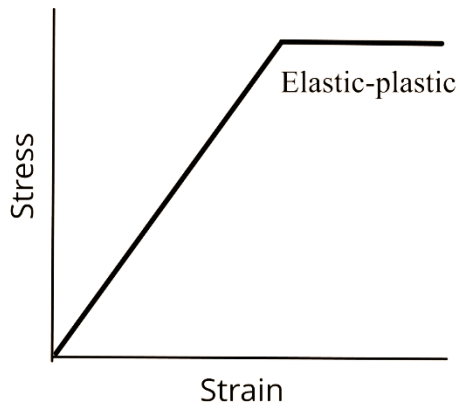
Figure 13: Guidelines for the selection of modulus ratio (MR) values in Equation (21) - based on Deere (1968) and Palmstrom and Singh (2001).



a) Very good quality hard rock mass



b) Average quality hard rock mass



c) Poor quality hard rock mass

Figure 14: Suggested post failure characteristics for different quality rock masses.

Reliability of rock mass strength estimates

The techniques described in the preceding sections of this chapter can be used to estimate the strength and deformation characteristics of isotropic jointed rock masses. When applying this procedure to rock engineering design problems, most users consider only the ‘average’ or mean properties. In fact, all these properties exhibit a distribution about the mean, even under the most ideal conditions, and these distributions can have a significant impact upon the design calculations.

In the text that follows, a slope stability calculation and a tunnel support design calculation are carried out to evaluate the influence of these distributions. In each case the strength and deformation characteristics of the rock mass are estimated by means of the Hoek-Brown procedure, assuming that the three input parameters are defined by normal distributions.

Input parameters

Figure 15 has been used to estimate the value of GSI from field observations of the block size, shape and discontinuity surface conditions. Included in this figure is a cross-hatched circle representing the 90% confidence limits of a GSI value of 25 ± 5 (equivalent to a standard deviation of approximately 2.5). This represents the range of values that an experienced geologist would assign to a rock mass described as BLOCKY/DISTURBED or DISINTEGRATED and POOR. Typically, rocks such as flysch, schist and some phyllites may fall within this range of rock mass descriptions.

In the author’s experience, some geologists go to extraordinary lengths to try to determine an ‘exact’ value of GSI. Geology does not lend itself to such precision and it is simply not realistic to assign a single value. A range of values, such as that illustrated in Figure 15 is more appropriate. In fact, in some complex geological environments, the range indicated by the cross-hatched circle may be too optimistic.

The two laboratory properties required for the application of the Hoek-Brown criterion are the uniaxial compressive strength of the intact rock (σ_{ci}) and the intact rock material constant m_i . Ideally these two parameters should be determined by triaxial tests on carefully prepared specimens as described by Hoek and Brown (1997).

The standard deviations assigned to these three distributions are based upon the author’s experience of geotechnical programs for major civil and mining projects where adequate funds are available for high quality investigations. For preliminary field investigations or ‘low budget’ projects, it is prudent to assume larger standard deviations for the input parameters.

It is assumed that all three input parameters (GSI, σ_{ci} and m_i) can be represented by normal distributions as illustrated in Figure 16.

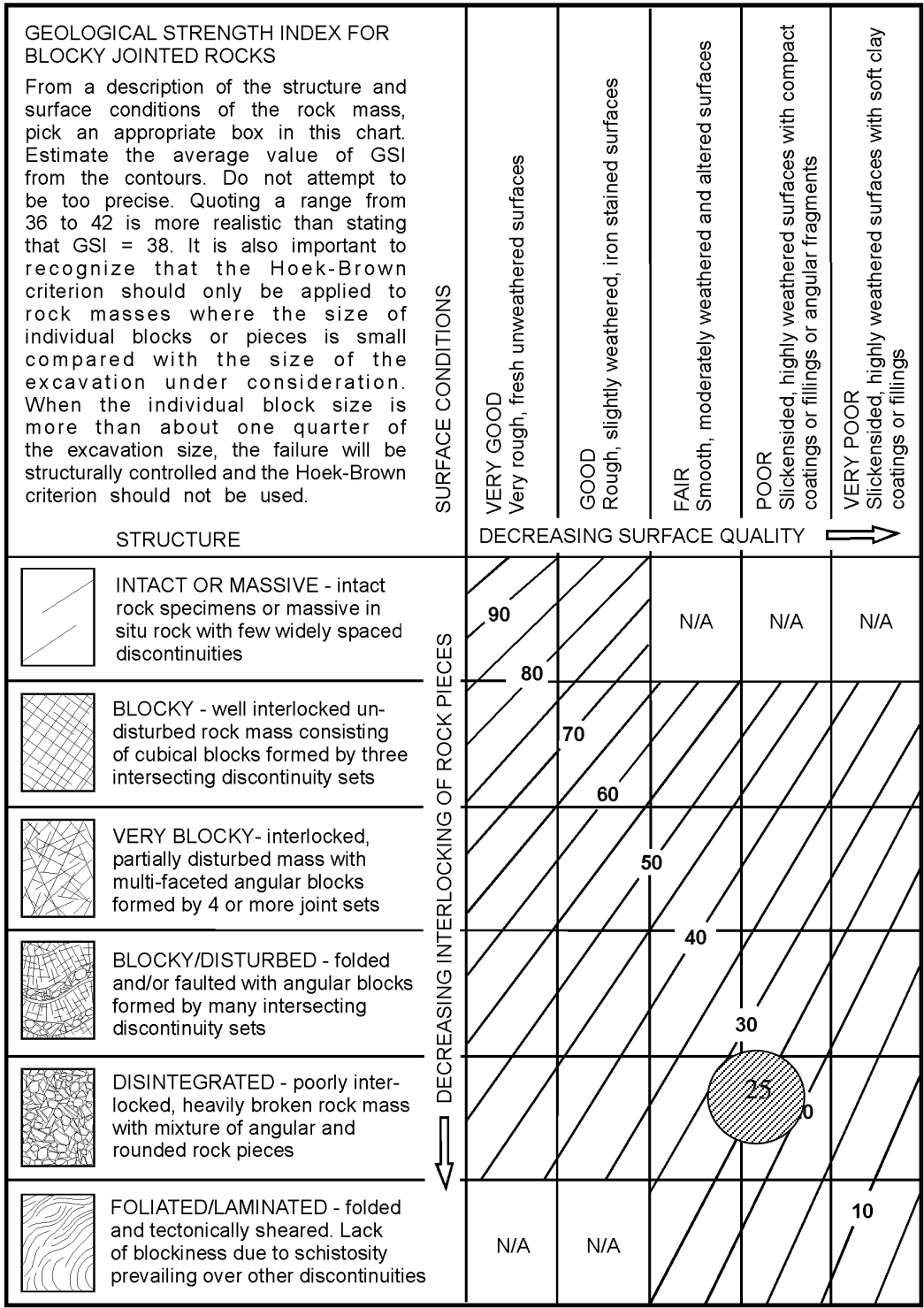


Figure 15: Estimate of Geological Strength Index GSI based on geological descriptions.

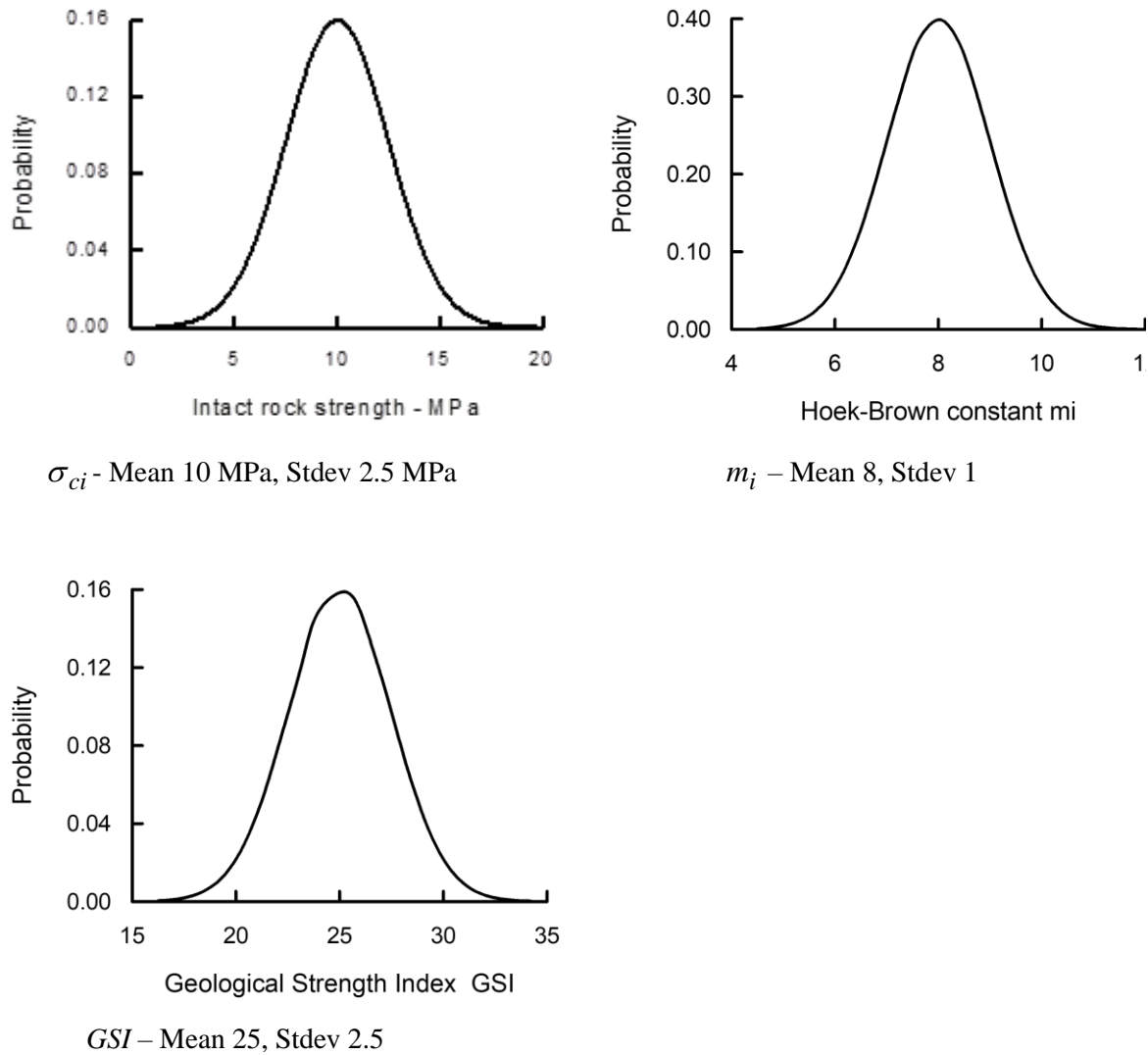
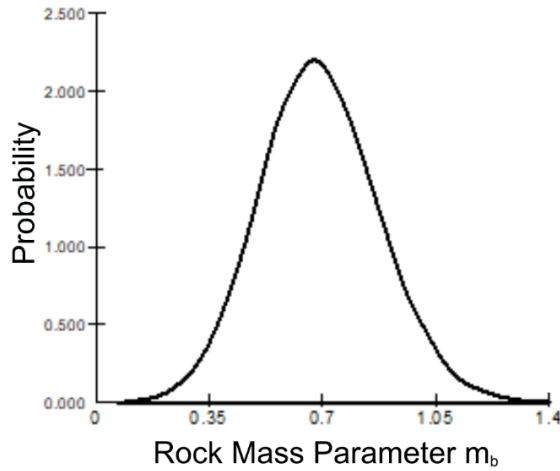
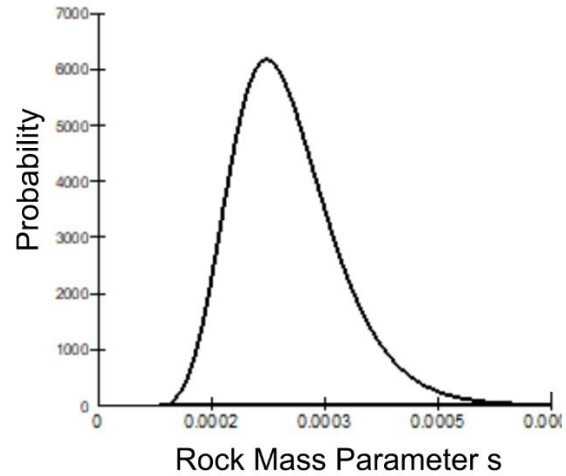


Figure 16: Assumed normal distributions for input parameters.

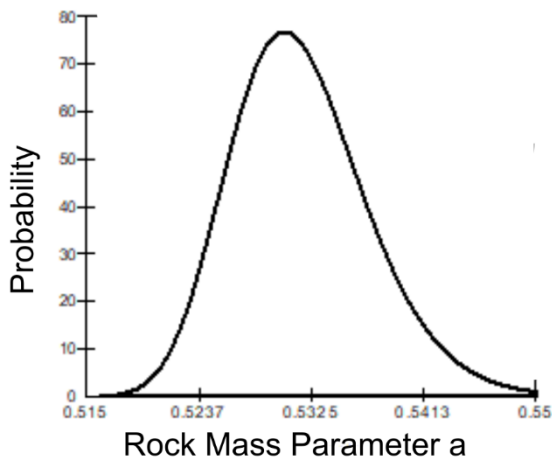
Note that where software programs will accept input in terms of the Hoek-Brown criterion directly, it is preferable to use this input rather than estimates of Mohr Coulomb parameters c and ϕ given by equations 11 and 12 on page 14. This eliminates the uncertainty associated with estimating equivalent Mohr-Coulomb parameters, as described above, and allows the program to compute the conditions for failure at each point directly from the curvilinear Hoek-Brown relationship. In addition, the input parameters for the Hoek-Brown criterion (m_i , s , and a) are independent variables and can be treated as such in any probabilistic analysis. On the other hand, the Mohr Coulomb c and ϕ parameters are correlated, which results in an additional complication in probabilistic analyses.



m_b - Mean 0.689, Stdev 0.183



s - Mean 0.00025, Stdev 0.00007



a - Mean 0.532, Stdev 0.00535

Figure 17: Calculated distributions for rock mass parameters.

Based on the three normal distributions for GSI, σ_{ci} and m_i given in Figure 16, distributions for the rock mass parameters m_b , s and a can be determined by a variety of methods. One of the simplest is to use a Monte Carlo simulation in which the distributions given in Figure 12 are used as input for equations 6, 7 and 8 to determine distributions for m_i , s and a . The results of such an analysis, using the Excel add-in @RISK (available from www.palisade.com), are given in Figure 17.

Slope stability calculation

To assess the impact of the variation in rock mass parameters, illustrated in Figures 16 and 17, a calculation of the factor of safety for a homogeneous slope was carried out using Bishop's circular failure analysis in the program SLIDE (available from www.roscience.com). The geometry of the slope and the phreatic surface are shown in Figure 18. The probabilistic option offered by the program was used and the rock mass properties were input as follows:

Property	Distribution	Mean	Std. dev.	Min*	Max*
m_b	Normal	0.6894	0.1832	0.0086	1.44
s	Lognormal	0.0002498	0.0000707	0.0000886	0.000704
a	Normal	0.5317	0.00535	0.5171	0.5579
σ_{ci}	Normal	10000 kPa	2500 kPa	1000 kPa	20000 kPa
Unit weight γ		23 kN/m ³			

* Note that, in SLIDE, these values are input as relative proportions of the mean value and not as the absolute values shown here.

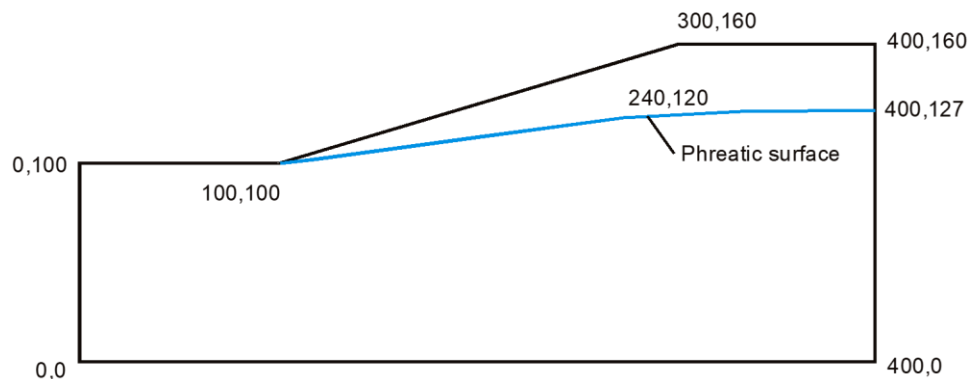


Figure 18: Slope and phreatic surface geometry for a homogeneous slope.

The distribution of the calculated factor of safety is shown in Figure 19 and it was found that this is best represented by a beta distribution with a mean value of 2.998, a standard deviation of 0.385, a minimum value of 1.207 and a maximum value of 4.107. There is zero probability of failure for this slope as indicated by the minimum factor of safety of 1.207. All critical failure surface exit at the toe of the slope.

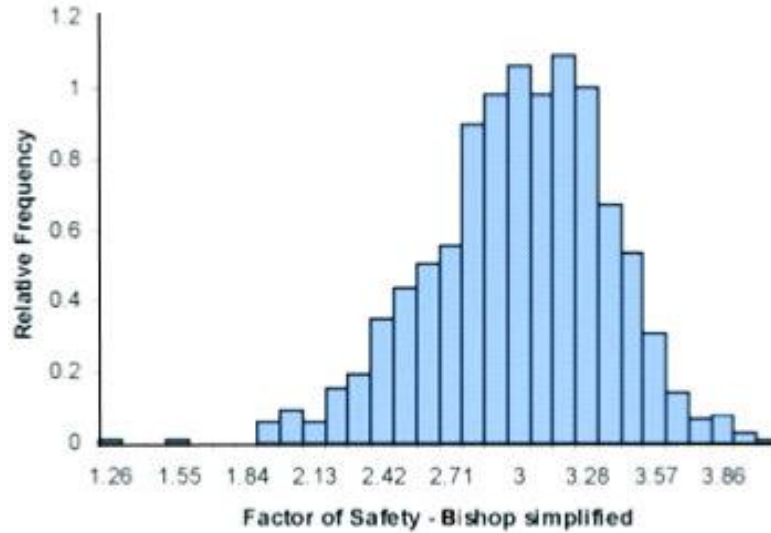


Figure 19: Distribution of factors of safety for the slope shown in Figure 18 from a probabilistic analysis using the program SLIDE.

Consider a circular tunnel, illustrated in Figure 20, with a radius r_o in a stress field in which the horizontal and vertical stresses are both p_o . If the stresses are high enough, a ‘plastic’ zone of damaged rock of radius r_p surrounds the tunnel. A uniform support pressure p_i is provided around the perimeter of the tunnel.

A probabilistic analysis of the behaviour of this tunnel was carried out using the program RocSupport (available from www.rocscience.com) with the following input parameters:

Property	Distribution	Mean	Std. dev.	Min*	Max*
Tunnel radius r_o		5 m			
In situ stress p_o		2.5 MPa			
m_b	Normal	0.6894	0.1832	0.0086	1.44
s	Lognormal	0.0002498	0.0000707	0.0000886	0.000704
a	Normal	0.5317	0.00535	0.5171	0.5579
σ_{ci}	Normal	10 MPa	2.5 MPa	1 MPa	20 MPa
E		1050 MPa			

* Note that, in RocSupport, these values are input as values relative to the mean value and not as the absolute values shown above.

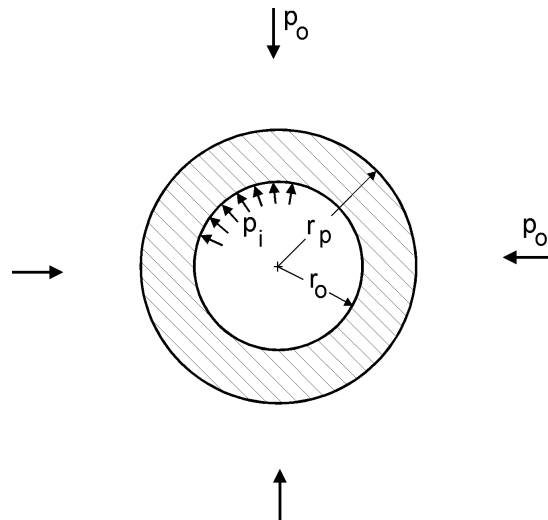


Figure 20: Development of a plastic zone around a circular tunnel in a hydrostatic stress field.

The resulting characteristic curve or support interaction diagram is presented in Figure 21. This diagram shows the tunnel wall displacements induced by progressive failure of the rock mass surrounding the tunnel as the face advances. The support is provided by a 5 cm shotcrete layer with 15 cm wide flange steel ribs spaced 1 m apart. The support is assumed to be installed 2 m behind the face after a wall displacement of 25 mm or a tunnel convergence of 50 mm has occurred. At this stage the shotcrete is assigned a 3-day compressive strength of 11 MPa.

The Factor of Safety of the support system is defined by the ratio of support capacity to demand as defined in Figure 21. The capacity of the shotcrete and steel set support is 0.4 MPa and it can accommodate a tunnel convergence of approximately 30 mm. As can be seen from Figure 21, the mobilised support pressure at equilibrium (where the characteristic curve and the support reaction curves cross) is approximately 0.15 MPa. This gives a first deterministic estimate of the Factor of Safety as 2.7.

The probabilistic analysis of the factor of safety yields the histogram shown in Figure 22. A Beta distribution is found to give the best fit to this histogram and the mean Factor of Safety is 2.73, the standard deviation is 0.46, the minimum is 2.23 and the maximum is 9.57.

This analysis assumes that the tunnel is circular, the rock mass is homogeneous and isotropic, the in-situ stresses are equal in all directions and the support is placed as a closed circular ring. These assumptions are seldom valid for actual tunnelling conditions and hence the analysis described above should only be used as a first rough approximation in design. Where the analysis indicates that tunnel stability is likely to be a problem, it is essential that a more detailed numerical analysis, considering actual tunnel geometry and rock mass conditions, should be carried out.

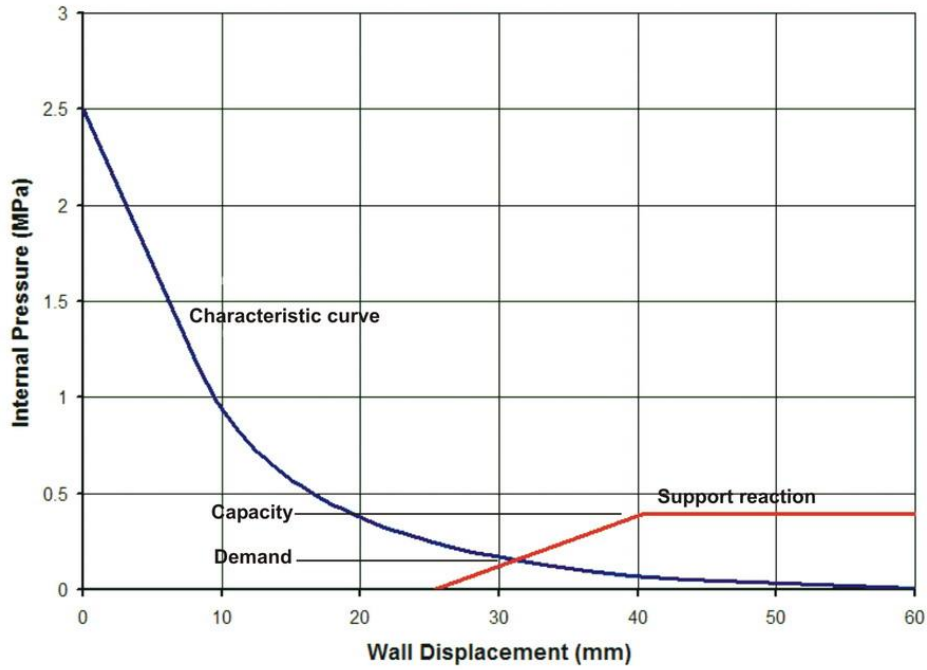


Figure 21: Rock support interaction diagram for a 10 m diameter tunnel subjected to a uniform in situ stress of 2.5 MPa.

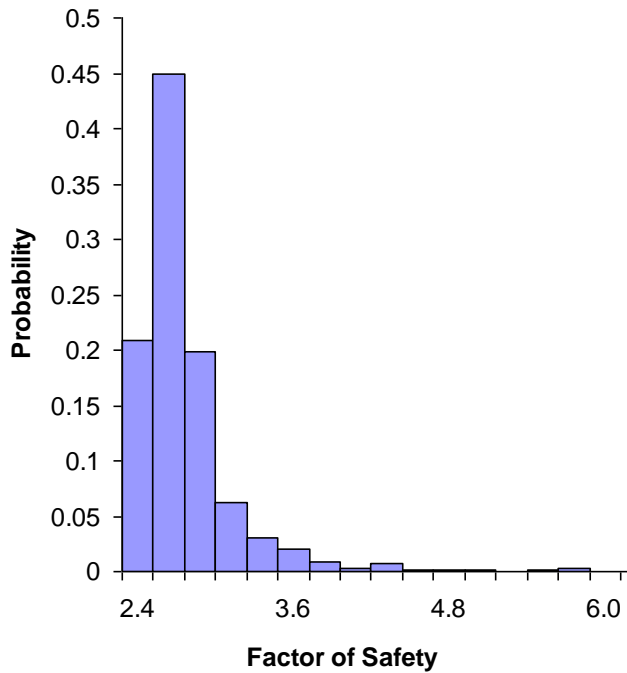


Figure 22: Distribution of the Factor of Safety for the tunnel discussed above.

Conclusions

The uncertainty associated with estimating the properties of in situ rock masses has a significant impact on the design of slopes and excavations in rock. The examples that have been explored in this section show that, even when using the ‘best’ estimates currently available, the ranges of calculated factors of safety are uncomfortably large. These ranges become alarmingly large when poor site investigation techniques and inadequate laboratory procedures are used.

Given the inherent difficulty of assigning reliable numerical values to rock mass characteristics, it is unlikely that ‘accurate’ methods for estimating rock mass properties will be developed in the foreseeable future. Consequently, the user of the Hoek-Brown procedure or of any other equivalent procedure for estimating rock mass properties should not assume that the calculations produce unique reliable numbers. The simple techniques described in this section can be used to explore the possible range of values and the impact of these variations on engineering design.

Practical examples of rock mass property estimates

The following examples are presented to illustrate the range of rock mass properties that can be encountered in the field and to give the reader some insight of how the estimation of rock mass properties was tackled in several actual projects.

Massive weak rock

Karzulovic and Diaz (1994) have described the results of a program of triaxial tests on a cemented breccia known as Braden Breccia from the El Teniente mine in Chile. To design underground openings in this rock, attempts were made to classify the rock mass in accordance with Bieniawski’s RMR system. However, as illustrated in Figure 23, this rock mass has very few discontinuities and so assigning realistic numbers to terms depending upon joint spacing and condition proved to be very difficult. Finally, it was decided to treat the rock mass as a weak but homogeneous ‘almost intact’ rock, like a weak concrete, and to determine its properties by means of triaxial tests on large diameter specimens.

A series of triaxial tests was carried out on 100 mm diameter core samples, illustrated in Figure 24. The results of these tests were analysed by means of the regression analysis using the program RocLab. Back analysis of the behaviour of underground openings in this rock indicate that the in-situ GSI value is approximately 75. From RocLab the following parameters were obtained:

Intact rock strength	σ_{ci}	51 MPa	Hoek-Brown constant	m_b	6.675
Hoek-Brown constant	m_i	16.3	Hoek-Brown constant	s	0.062
Geological Strength Index	GSI	75	Hoek-Brown constant	a	0.501
			Deformation modulus	E_m	15000 MPa



Figure 23: Braden Breccia at El Teniente Mine in Chile. This rock is a cemented breccia with practically no joints. It was dealt with in a manner like weak concrete and tests were carried out on 100 mm diameter specimens illustrated in Figure 24.



Figure 24. 100 mm diameter by 200 mm long specimens of Braden Breccia from the El Teniente mine in Chile.

Massive strong rock masses

The Rio Grande Pumped Storage Project in Argentina includes a large underground powerhouse, a surge control complex and a 6 km long tailrace tunnel. The rock mass surrounding these excavations is massive gneiss with very few joints. A typical core from this rock mass is illustrated in Figure 25. The appearance of the rock at the surface was illustrated earlier in Figure 8, which shows a cutting for the dam spillway.



Figure 25: Excellent quality core with very few discontinuities from the massive gneiss of the Rio Grande project in Argentina.



Figure 26: Top heading of the 12 m span, 18 m high tailrace tunnel for the Rio Grande Pumped Storage Project.

The rock mass can be described as BLOCKY/VERY GOOD and the GSI value, from Figure 6, is 75. Typical characteristics for the rock mass are as follows:

Intact rock strength	σ_{ci}	110 MPa	Hoek-Brown constant	m_b	11.46
Hoek-Brown constant	m_i	28	Hoek-Brown constant	s	0.062
Geological Strength Index	GSI	75	Constant	a	0.501
			Deformation modulus	E_m	45000 MPa

Figure 26 illustrates the 8 m high 12 m span top heading for the tailrace tunnel. The final tunnel height of 18 m was achieved by blasting two 5 m high benches. The top heading was excavated by full-face drill and blast and, because of the excellent quality of the rock mass and the tight control on blasting quality, most of the top heading did not require any support.

Details of this project are to be found in Moretto et al (1993). Hammett and Hoek (1981) have described the design of the support system for the 25 m span underground powerhouse in which a few structurally controlled wedges were identified and stabilised during excavation. This cavern has performed for more than 40 years without stability problems.

Average quality rock mass

The partially excavated powerhouse cavern in the Nathpa Jhakri Hydroelectric project in Himachel Pradesh, India, is illustrated in Figure 26. The rock is a jointed quartz mica schist, which has been extensively evaluated by the Geological Survey of India as described by Jalote et al (1996). An average GSI value of 65 was chosen to estimate the rock mass properties which were used for the cavern support design. Additional support, installed on the instructions of the engineers, was placed in weaker rock zones.

The assumed rock mass properties are as follows:

Intact rock strength	σ_{ci}	30 MPa	Hoek-Brown constant	m_b	4.3
Hoek-Brown constant	m_i	15	Hoek-Brown constant	s	0.02
Geological Strength Index	GSI	65	Constant	a	0.5
			Deformation modulus	E_m	10000 MPa

Two- and three-dimensional stress analyses of the nine stages used to excavate the cavern were carried out to determine the extent of potential rock mass failure and to provide guidance in the design of the support system. An isometric view of one of the three-dimensional models is given in Figure 27.



Figure 26: Partially completed 20 m span, 42.5 m high underground powerhouse cavern of the Nathpa Jhakri Hydroelectric Project in Himachel Pradesh, India. The cavern is approximately 300 m below the surface.

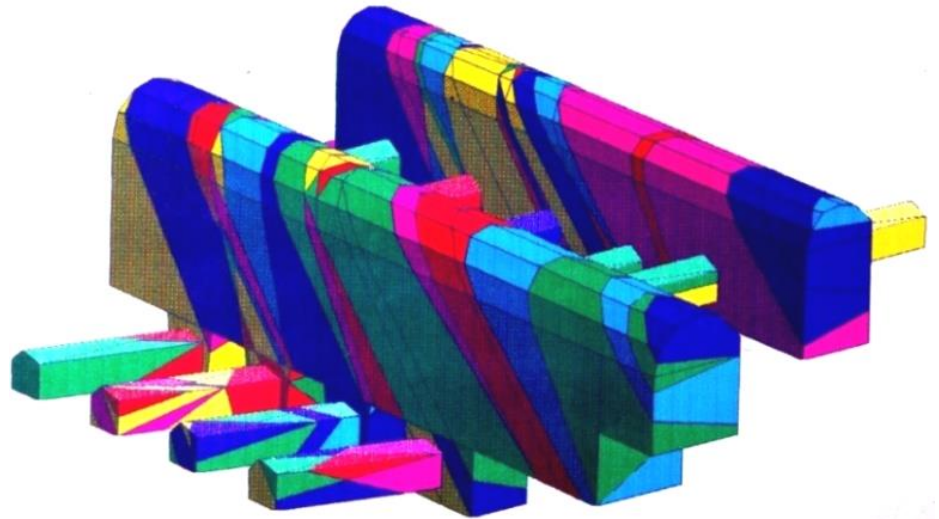


Figure 27: Isometric view of the 3DEC model of the underground powerhouse cavern and the transformer gallery of the Nathpa Jhakri Hydroelectric Project, analysed by Dr. B. Dasgupta.

The support for the powerhouse cavern consists of rockbolts and mesh reinforced shotcrete. Alternating 6 and 8 m long 32 mm diameter bolts on 1 x 1 m and 1.5 x 1.5 m centres are used in the arch. Alternating 9 and 7.5 m long 32 mm diameter bolts were used in the upper and lower sidewalls with alternating 9 and 11 m long 32 mm rockbolts in the centre of the sidewalls, all at a grid spacing of 1.5 m. Shotcrete consists of two 50 mm thick layers of plain shotcrete with an interbedded layer of weldmesh. The support provided by the shotcrete was not included in the support design analysis, which relies upon the rockbolts to provide all the support required.

In the headrace tunnel, some zones of sheared quartz mica schist were encountered, which resulted in large displacements as illustrated in Figure 28. This is a common problem in hard rock tunnelling where the excavation sequence and support system have been designed for 'average' rock mass conditions. Unless very rapid changes in the length of blast rounds and the installed support are made when an abrupt change to poor rock conditions occurs, for example when a fault is encountered, problems with controlling tunnel deformation can arise.

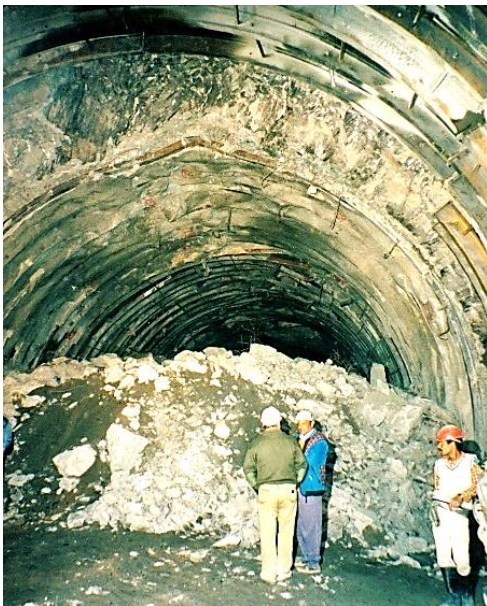


Figure 28: Large displacements in the top heading of the headrace tunnel of the Nathpa Jhakri Hydroelectric project. Displacements are the result of deteriorating rock mass quality when tunnelling through a fault zone.

The only effective way to anticipate this type of problem is to probe ahead of the advancing face. Typically, a long probe hole is percussion drilled during a maintenance shift and the penetration rate, return water flow and chippings are constantly monitored during drilling. Where significant problems are indicated by this percussion drilling, one or two diamond-drilled holes may be required to investigate these problems in more detail. In some special cases, the use of a pilot tunnel may be more effective in that it permits the ground properties to be defined more accurately than is possible with probe hole drilling. In addition, pilot tunnels allow pre-drainage and pre-reinforcement of the rock ahead of the development of the full excavation profile.

Poor quality rock mass at shallow depth

Kavvadas et al (1996) have described some of the geotechnical issues associated with the construction of 18 km of tunnels and the 21 underground stations of the Athens Metro. These excavations are all shallow with typical depths to tunnel crown of between 15 and 20 m. The principal problem is one of surface subsidence rather than failure of the rock mass surrounding the openings.

The rock mass is locally known as Athenian schist which is a term used to describe a sequence of Upper Cretaceous flysch-type sediments including thinly bedded clayey and calcareous sandstones, siltstones (greywackes), slates, shales, and limestones. During the Eocene, the Athenian schist formations were subjected to intense folding and thrusting. Later extensive faulting caused extensional fracturing and widespread weathering and alteration of the deposits.

The GSI values range from approximately 15 to 45. The higher values correspond to the intercalated layers of sandstones and limestones, which can be described as BLOCKY/DISTURBED and POOR (Figure 6). The completely decomposed schist can be described as DISINTEGRATED and VERY POOR and has GSI values ranging from 15 to 20. Rock mass properties for the completely decomposed schist, using a GSI value of 20, are as follows:

Intact rock strength - MPa	σ_{ci}	5-10	Hoek-Brown constant	m_b	0.55
Hoek-Brown constant	m_i	9.6	Hoek-Brown constant	s	0.0001
Geological Strength Index	GSI	20	Hoek-Brown constant	a	0.544
			Deformation modulus	E_m	600 MPa

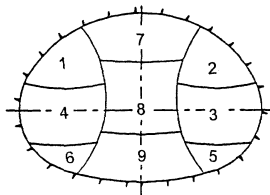


Figure 29: Twin side drift and central pillar excavation method. Temporary support consists of double wire mesh reinforced 250 - 300 mm thick shotcrete shells with embedded lattice girders or HEB 160 steel sets at 0.75 - 1 m spacing.

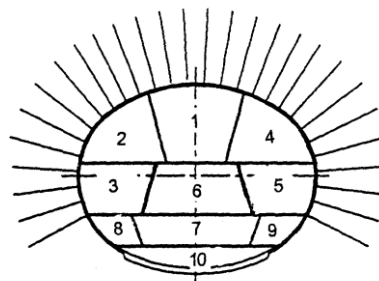


Figure 30: Top heading and bench method of excavation. Temporary support consists of a 200 mm thick shotcrete shell with 4 and 6 m long untensioned grouted rockbolts at 1.0 - 1.5 m spacing.

The Academia, Syntagma, Omonia and Olympion stations were constructed using the New Austrian Tunnelling Method twin side drift and central pillar method as illustrated in Figure 29. The more conventional top heading and bench method, illustrated in Figure 30, was used for the excavation of the Ambelokipi station. These stations are all 16.5 m wide and 12.7 m high. The appearance of the rock mass in one of the Olympion station side drift excavations is illustrated in Figure 31.



Figure 31: Appearance of the very poor-quality Athenian Schist at the face of the side heading illustrated in Figure 29.

Numerical analyses of the two excavation methods showed that the twin side drift method resulted in slightly less rock mass failure in the crown of the excavation. However, the final surface displacements induced by the two excavation methods were practically identical.

Maximum vertical displacements of the surface above the centreline of the Omonia station amounted to 51 mm. Of this, 28 mm occurred during the excavation of the side drifts, 14 mm during the removal of the central pillar and a further 9 mm occurred as a time dependent settlement after completion of the excavation. According to Kavvadas et al (1996), this time dependent settlement is due to the dissipation of excess pore water pressures which were built up during excavation. In the case of the Omonia station, the excavation of recesses towards the eastern end of the station, after completion of the station excavation, added a further 10 to 12 mm of vertical surface displacement at this end of the station.

Poor quality rock mass under high stress

The Yacambú Quibor tunnel in Venezuela is one of the most difficult tunnels in the world. This 25 km long water supply tunnel, through the Andes, is being excavated in sandstones and phyllites at depths of up to 1200 m below surface. The graphitic phyllite is a very poor-quality rock and gives rise to serious squeezing problems which, without adequate support, result in complete closure of the tunnel. A full-face tunnel-boring machine was destroyed in 1979 when trapped by squeezing ground conditions.

The graphitic phyllite has an average unconfined compressive strength of about 50 MPa and the estimated GSI value is about 25 (see Figures 2 and 3). Typical rock mass properties are as follows:

Intact rock strength MPa	σ_{ci}	50	Hoek-Brown constant	m_b	0.481
Hoek-Brown constant	m_i	10	Hoek-Brown constant	s	0.0002
Geological Strength Index	GSI	25	Hoek-Brown constant	a	0.53
			Deformation modulus MPa	E_m	1000

Various support methods were used on this tunnel and only one will be considered here. This was a trial section of tunnel, at a depth of approximately 600 m, constructed in 1989. The support of the 5.5 m span tunnel was by means of a complete ring of 5 m long, 32 mm diameter untensioned grouted dowels with a 200 mm thick shell of reinforced shotcrete. This support system proved to be very effective but was later abandoned in favour of yielding steel sets (steel sets with sliding joints) because of construction schedule considerations. In fact, at a depth of 1200 m below surface (2004-2006) it is doubtful if the rockbolts would have been effective because of the very large deformations that could only be accommodated by steel sets with sliding joints.

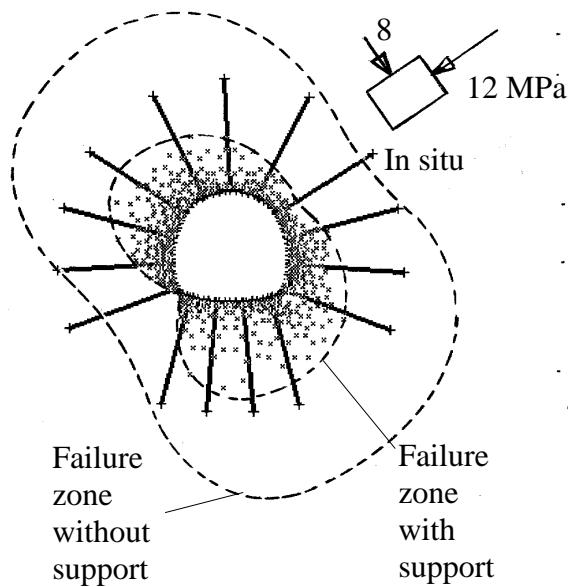


Figure 33: Results of a numerical analysis of the failure of the rock mass surrounding the Yacambu-Quibor tunnel when excavated in graphitic phyllite at a depth of approximately 600 m below surface.

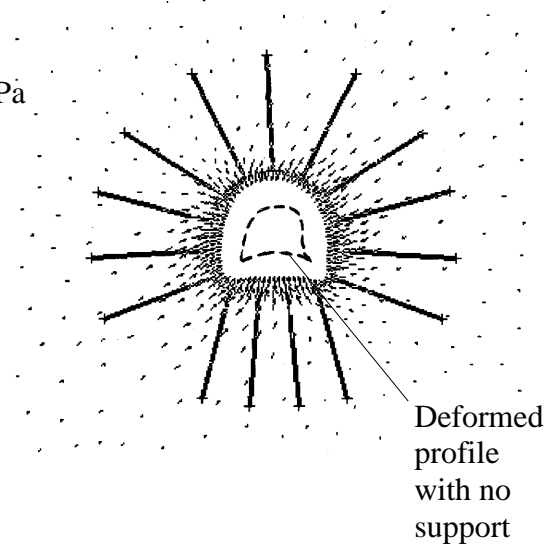


Figure 34: Displacements in the rock mass surrounding the Yacambu-Quibor tunnel. The maximum calculated displacement is 258 mm with no support and 106 mm with support.

Examples of the results of a typical numerical stress analysis of this trial section, carried out using the program PHASE2, are given in Figures 33 and 34. Figure 33 shows the extent of failure, with and without support, while Figure 34 shows the displacements in the rock mass surrounding the tunnel. Note that the criteria used to judge the effectiveness of the support design are that the zone of failure surrounding the tunnel should lie within the envelope of the rockbolt support, the rockbolts should not be stressed to failure and the displacements should be of reasonable magnitude and should be uniformly distributed around the tunnel. All these objectives were achieved by the support system described earlier.

Slope stability considerations

When dealing with slope stability problems in rock masses, great care must be taken in attempting to apply the Hoek-Brown failure criterion, particularly for small, steep slopes. As illustrated in Figure 35, even rock masses that appear to be good candidates for the application of the criterion can suffer shallow structurally controlled failures under the very low stress conditions which exist in such slopes.



Figure 35: Structurally controlled failure in the face of a steep bench in a heavily jointed rock mass.

As a rule, when designing slopes in rock, the initial approach should always be to search for potential failures controlled by adverse structural conditions. These may take the form of planar failures on outward dipping features, wedge failures on intersecting features, toppling failures on inward dipping failures or complex failure modes involving all these processes. Only when the potential for structurally controlled failures has been eliminated, should consideration be given to treating the rock mass as an isotropic material as required by the Hoek-Brown failure criterion.

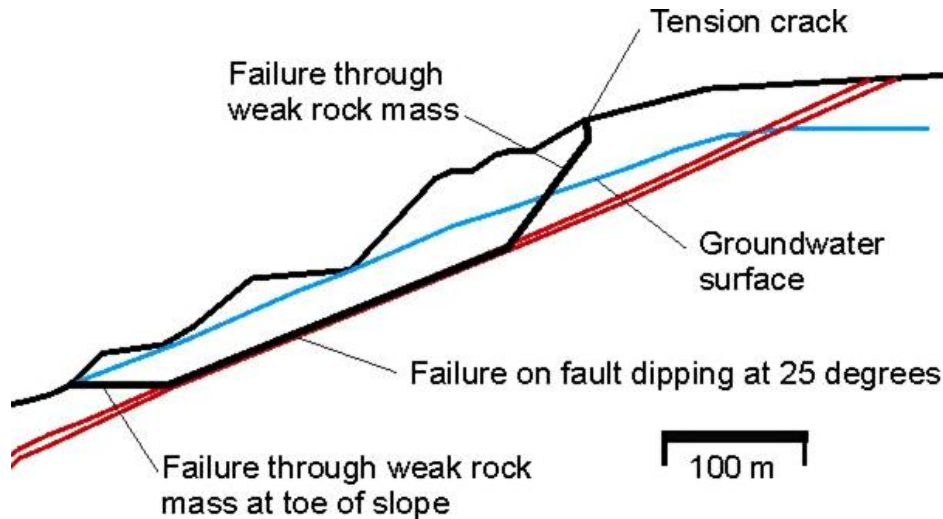


Figure 36: Complex slope failure controlled by an outward dipping basal fault and circular failure through the poor-quality rock mass overlying the toe of the slope.

Figure 36 illustrates a case in which the base of a slope failure is defined by an outward dipping fault that does not daylight at the toe of the slope. Circular failure through the poor-quality rock mass overlying the fault allows failure of the toe of the slope. Analysis of this problem was carried out by assigning the rock mass at the toe properties that had been determined by application of the Hoek-Brown criterion. A search for the critical failure surface was carried out utilising the program SLIDE which allows complex failure surfaces to be analysed and which includes facilities for the input of the Hoek-Brown failure criterion.

References

- Balmer, G. 1952. A general analytical solution for Mohr's envelope. *Am. Soc. Test. Mat.* 52, 1260-1271.
- Bieniawski, Z.T. 1976. Rock mass classification in rock engineering. *In Exploration for rock engineering*, proc. of the symp., (ed. Z.T. Bieniawski) 1, 97-106. Cape Town: Balkema.
- Bieniawski, Z.T. 1989. *Engineering rock mass classifications*. New York: Wiley.
- Deere D.U. 1968. Chapter 1: Geological considerations. In *Rock Mechanics in Engineering Practice* (eds. Stagg K.G. and Zienkiewicz, O.C.), 1-20. London: John Wiley and Sons.
- Franklin, J.A. and Hoek, E. 1970. Developments in triaxial testing equipment. *Rock Mech.* 2, 223-228. Berlin: Springer-Verlag.
- Hammett, R.D. and Hoek, E. 1981. Design of large underground caverns for hydro-electric projects, with reference to structurally controlled failure mechanisms. *Proc. American Soc. Civil Engrs. Int. Conf. on recent developments in geotechnical engineering for hydro projects*. 192-206. New York: ASCE
- Hoek, E. 1983. Strength of jointed rock masses, 23rd. Rankine Lecture. *Géotechnique* 33(3), 187-223.
- Hoek, E. 1994. Strength of rock and rock masses, *ISRM News Journal*, 2(2), 4-16.
- Hoek, E. and Brown, E.T. 1980a. *Underground excavations in rock*. London: Instn Min. Metall.
- Hoek, E. and Brown, E.T. 1980b. Empirical strength criterion for rock masses. J. *Geotech. Engng Div., ASCE* 106(GT9), 1013-1035.
- Hoek, E. and Brown, E.T. 1988. The Hoek-Brown failure criterion - a 1988 update. In *Rock engineering for underground excavations, proc. 15th Canadian rock mech. symp.*, (ed. J.C. Curran), 31-38. Toronto: Dept. Civ. Eng University of Toronto.
- Hoek, E., Marinos, P. and Benissi, M. 1998. Applicability of the Geological Strength Index (GSI) classification for very weak and sheared rock masses. The case of the Athens Schist Formation. *Bull. Engng. Geol. Env.* 57(2), 151-160.
- Hoek, E. and Brown, E.T. 1997. Practical estimates of rock mass strength. *Int. J. Rock Mech. Mining Sci. & Geomech. Abstr.* 34(8), 1165-1186.
- Hoek, E., Kaiser, P.K. and Bawden, W.F. 1995. *Support of underground excavations in hard rock*. Rotterdam: Balkema.
- Hoek, E., Wood, D. and Shah, S. 1992. A modified Hoek-Brown criterion for jointed rock masses. *Proc. rock characterization, symp. Int. Soc. Rock Mech.*: Eurock '92, (ed. J.A. Hudson), 209-214. London: Brit. Geol. Soc.

- Hoek E, Carranza-Torres CT, Corkum B. Hoek-Brown failure criterion-2002 edition. In: *Proceedings of the 5th North American Rock Mechanics Symp.*, Toronto, Canada, 2002: 1: 267–73.
- Hoek, E., Marinos, P., Marinos, V. 2005. Characterization and engineering properties of tectonically undisturbed but lithologically varied sedimentary rock masses. *Int. J. Rock Mech. Min. Sci.*, 42/2, 277-285.
- Hoek, E and Diederichs, M. 2006. Empirical estimates of rock mass modulus. *Int. J Rock Mech. Min. Sci.*, 43, 203–215.
- Hoek, E. and Brown, E.T. 2019. The Hoek-Brown criterion and GSI -2018 edition. *Journal of Rock Mechanics and Geotechnical Engineering*. 2019; 6(3): 445-463.
- Karzulovic A. and Díaz, A.1994. Evaluación de las Propiedades Geomacánicas de la Brecha Braden en Mina El Teniente. *Proc. IV Congreso Sudamericano de Mecánica de Rocas*, Santiago 1, 39-47.
- Kavvadas M., Hewison L.R., Lastaratos P.G., Seferoglou, C. and Michalis, I. 1996. Experience in the construction of the Athens Metro. *Proc. Int. symp. geotechnical aspects of underground construction in soft ground*. (Eds Mair R.J. and Taylor R.N.), 277-282. London: City University.
- Jalote, P.M., Kumar A. and Kumar V. 1996. Geotechniques applied in the design of the machine hall cavern, Nathpa Jhakri Hydel Project, N.W. Himalaya, India. *J. Engng Geol. (India)* XXV(1-4), 181-192.
- Marinos, P, and Hoek, E. 2001. Estimating the geotechnical properties of heterogeneous rock masses such as flysch. *Bull. Engng Geol. & the Environment (IAEG)*, 60, 85-92.
- Marinos, P., Hoek, E., Marinos, V. 2006. Variability of the engineering properties of rock masses quantified by the geological strength index: the case of ophiolites with special emphasis on tunnelling. *Bull. Eng. Geol. Env.*, 65/2, 129-142.
- Moretto O., Sarra Pistone R.E. and Del Rio J.C. 1993. A case history in Argentina - Rock mechanics for underground works in the pumping storage development of Rio Grande No 1. In *Comprehensive Rock Engineering*. (Ed. Hudson, J.A.) 5, 159-192. Oxford: Pergamon.
- Palmstrom A. and Singh R. 2001. The deformation modulus of rock masses: comparisons between in situ tests and indirect estimates. *Tunnelling and Underground Space Technology*. 16: 115-131.
- Salcedo D.A.1983. Macizos Rocosos: Caracterización, Resistencia al Corte y Mecanismos de Rotura. *Proc. 25 Aniversario Conferencia Soc. Venezolana de Mecánica del Suelo e Ingeniería de Fundaciones*, Caracas. 143-172.